ISSN 0021-3640, JETP Letters, 2023, Vol. 117, No. 7, pp. 540–545. © The Author(s), 2023. This article is an open access publication.
Russian Text © The Author(s), 2023, published in Pis'ma v Zhurnal Eksperimental'noi i Teoreticheskoi Fiziki, 2023, Vol. 117, No. 7, pp. 543–549.

CONDENSED MATTER

Ultrasonic Spin Echo Caused by Irreversible Phase Relaxation

S. V. Sazonov[a, b, *]

[a] National Research Center Kurchatov Institute, Moscow, 123182 Russia

[b] Moscow Aviation Institute (National Research University), Moscow, 125993 Russia

*e-mail: sazonov.sergey@gmail.com

Received February 13, 2023; revised March 1, 2023; accepted March 1, 2023

The possibility of the generation of a primary ultrasonic echo in the system of equidistant Zeeman triplets owing to irreversible phase relaxation has been predicted. The disappearance of phase relaxation results in the disappearance of an echo signal. This effect is due to the destructive interference of two allowed quantum transitions emitting in antiphase. The difference between the phase relaxation times at these transitions leads to an incomplete quenching of resulting coherence, leading to generation of the echo signal.

DOI: 10.1134/S0021364023600490

1. INTRODUCTION

Echo phenomena are due to the coherence of atomic states, which is induced in a medium by various pulses. In the case of the photon echo, these are visible and infrared laser pulses [1–4]. In the case of nuclear and electron spin echo, the range of probe electromagnetic pulses is from radiofrequencies to microwave frequencies [5, 6]. The same frequency range of ultrasonic pulses is involved in the formation of the phonon echo in paramagnetic crystals [7–10].

Since echo signals hold memory on the prehistory of action on various media [3, 11], echo effects can be applied in information storage and processing systems.

To form echo signals, a medium is usually exposed to coherent classical pulses with a very narrow frequency spectrum. Femtosecond lasers allow one to use broadband probe pulses with a noise energy spectrum [12, 13]. Such incoherent signals also can induce coherence in atomic states of various media [14–16]. Echo responses to these signals are called incoherent echo [17–21]. In this case, pulses supplied to the medium are incoherent. Consequently, the following paradoxical question naturally arises: Can incoherent processes in the medium result in the appearance of coherent echo signals?

It is well known that irreversible phase relaxation destroys atomic coherent states. In particular, phase relaxation obviously reduces the intensity of echo responses in two-level atoms [3, 4]. Phase relaxation in multilevel media can be supplemented by the quantum interatomic interference of different quantum transitions. Therefore, nontrivial phenomena caused by the effect of phase relaxation on the properties of echo signals in the medium exposed to resonant coherent pulses can be expected.

The aim of this work is to study the role of irreversible phase relaxation in the formation of spin–phonon echo signals in a paramagnetic crystal exposed to coherent ultrasonic pulses.

2. BASIC EQUATIONS

Let a cubic crystal containing impurity paramagnetic ions be placed in the magnetic field **B**. It is known that paramagnetic ions with the effective spin $S = 1$ most strongly interact with vibrations of a crystal lattice [22]. In this case, Zeeman splitting results in the formation of a triplet of steady states with different projections $S_z = 0, \pm 1$ of the effective spin on the **B** direction taken as the z axis (Fig. 1). Let this z axis coincide with one of the fourth-order symmetry axes of the cubic crystal and ultrasonic pulses supplied to the medium propagate along the x axis perpendicular to the z axis. These shear strain pulses, being transverse, are polarized along the magnetic field.

The Hamiltonian for a single ion interacting with local deformations of the cubic crystal in the situation described above can be written in the form [22]

$$\hat{H} = \hbar\omega_0'\hat{S}_z + \hat{H}_{\text{int}}, \tag{1}$$

where $\hbar$ is the reduced Planck constant, ω_0' is the splitting frequency in the Zeeman triplet (Fig. 1), and $\hat{H}_{\text{int}}$ is the Hamiltonian describing the spin–phonon coupling represented as

$$\hat{H}_{\text{int}} = \frac{1}{2}G_{\perp}(\hat{S}_x\hat{S}_z + \hat{S}_z\hat{S}_x)\frac{\partial u_z}{\partial x}. \tag{2}$$

Here, $G_{\perp}$ is the spin–phonon coupling constant, u_z is the projection of the local displacement of sites of the

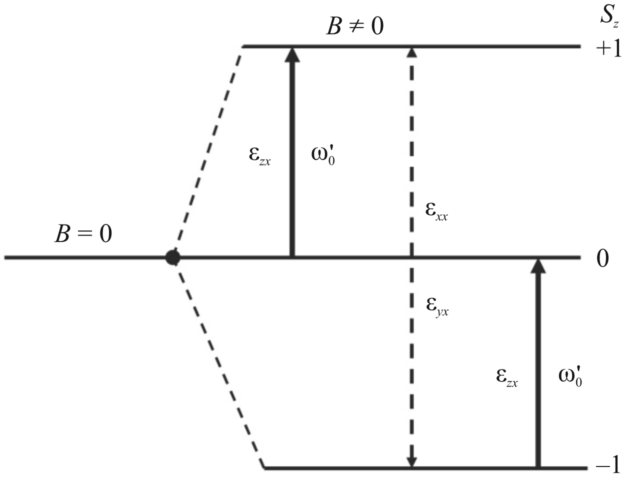

Fig. 1. Splitting of the quantum level of the paramagnetic ion with the effective spin $S = 1$ into three Zeeman sublevels. The thick arrows mark allowed spin–phonon transitions for transverse ultrasonic pulses ε_{zx} polarized along the magnetic field **B**. The dashed arrow marks spin–phonon transitions for the longitudinal (ε_{xx}) and transverse (ε_{yx}) ultrasonic pulses polarized perpendicular to the magnetic field **B**.

crystal lattice in the **B** direction, and $\hat{S}_x$ and $\hat{S}_z$ are the 3×3 matrices corresponding to the spin $S = 1$ [22]:

$$\hat{S}_x = \frac{1}{\sqrt{2}}\begin{pmatrix} 0 & 1 & 0 \\ 1 & 0 & 1 \\ 0 & 1 & 0 \end{pmatrix}, \quad \hat{S}_z = \begin{pmatrix} 1 & 0 & 0 \\ 0 & 0 & 0 \\ 0 & 0 & -1 \end{pmatrix}. \tag{3}$$

The spin–phonon coupling in this case is due to the van Vleck mechanism [10, 22]. According to this mechanism, local distortions of the crystal lattice induced by ultrasonic pulses lead to gradients of the crystal electric field. These gradients in turn initiate electric quadrupole transitions between Zeeman sublevels of the paramagnetic ion.

The density matrix for quantum states of the paramagnetic ion (Fig. 1) can be represented in the form

$$\hat{\rho} = \begin{pmatrix} \rho_{++} & \rho_{+0} & \rho_{+-} \\ \rho_{0+} & \rho_{00} & \rho_{0-} \\ \rho_{-+} & \rho_{-0} & \rho_{--} \end{pmatrix}. \tag{4}$$

Here, the superscripts +, 0, and – mark the z projections of the effective spin +1, 0, and –1. The diagonal matrix elements satisfy the condition $\rho_{++} + \rho_{00} + \rho_{--} = 1$.

Using Eqs. (1)–(4), we write the equations for the elements $\rho_{\mu\nu}$ $(\mu, \nu = -, 0, +)$ of the density matrix $\hat{\rho}$ in the form

$$\frac{\partial \rho_{\mu\nu}}{\partial t} = -i(\omega'_{\mu\nu} - i/T_{\mu\nu})\rho_{\mu\nu} - \frac{i}{\hbar}\left[\hat{H}_{\rm int}, \hat{\rho}\right]_{\mu\nu}. \tag{5}$$

Here, $\omega'_{+0} = \omega'_{0-} = \omega'_0$, $\omega'_{+-} = 2\omega'_0$, $\omega'_{++} = \omega'_{00} = \omega'_{--} = 0$, $T_{\mu\nu} = T_{\nu\mu}$ is the irreversible phase relaxation time on the $\mu \leftrightarrow \nu$ quantum transition, and the relaxation of the populations of stationary Zeeman states is neglected because the corresponding relaxation times are shorter than the phase relaxation times $T_{\mu\nu}$ [23]. In addition, it is assumed that the characteristic time Δt of the echo experiment is also much longer than the relaxation time of the populations of Zeeman sublevels.

Further, using the standard semiclassical approach, Eqs. (1) and (2) are supplemented with the classical Hamiltonian for the elastic strain field of transverse ultrasonic pulses $H_a = \int \mathcal{H}_a d^3\mathbf{r}$, where integration is performed over the entire volume of the medium and the Hamiltonian density $\mathcal{H}_a$ is given by the expression

$$\mathcal{H}_a = \frac{p_z^2}{2\rho} + \frac{\rho}{2}a_\perp^2\left(\frac{\partial u_z}{\partial x}\right)^2, \tag{6}$$

where ρ is the density of the medium, p_z is the z component of the momentum density of the local transverse displacement of the crystal, and $a_\perp$ is the speed of transverse sound in the medium surrounding the considered paramagnetic crystal.

Effects of propagation of ultrasound in the considered paramagnetic crystal are insignificant for the experimental detection of echo signals because this detection is usually carried out far from this crystal. For this reason, the Hamiltonian (6) includes the parameters of the medium between the paramagnetic crystal and the detector of echo signals.

We use the Hamiltonian equations for continuous media [24]

$$\begin{aligned} \frac{\partial p_z}{\partial t} &= -\frac{\delta}{\delta u_z}(H_a + \langle \hat{H}_{\rm int}\rangle), \\ \frac{\partial u_z}{\partial t} &= \frac{\delta}{\delta p_z}(H_a + \langle \hat{H}_{\rm int}\rangle). \end{aligned} \tag{7}$$

Here, $\langle \hat{H}_{\rm int}\rangle = {\rm Tr}(\hat{\rho}\hat{H}_{\rm int})$ is the quantum average of the Hamiltonian describing the interaction of the effective spin with the transverse strain field.

Using Eqs. (7) and (2)–(4), we obtain the wave equation

$$\begin{aligned} &\frac{\partial^2 \varepsilon_{zx}}{\partial t^2} - a_\perp^2 \frac{\partial^2 \varepsilon_{zx}}{\partial x^2} \\ &= \frac{nG_\perp}{8\sqrt{2}\rho}\frac{\partial^2}{\partial x^2}\int_{-\infty}^{+\infty}(\rho_{+0} + \rho_{0+} - \rho_{0-} - \rho_{-0})g(\Delta)d\Delta, \end{aligned} \tag{8}$$

where $\varepsilon_{zx} = 0.5\partial u_z/\partial x$ is the shear strain, n is the concentration of paramagnetic ions, $g(\Delta)$ is the inhomogeneous broadening contour function on the $- \leftrightarrow +$ quantum transition centered at the frequency ω_0, and

$\Delta = \omega_0' - \omega_0$ is the detuning of the $- \leftrightarrow 0$ and $0 \leftrightarrow +$ quantum transitions in the considered paramagnetic ion from the central frequency of the spectral line.

The inhomogeneous wave equation (8) describes the propagation of transverse ultrasound in the medium surrounding the paramagnetic crystal, which is a source of echo signals. The parameters of this source are included on the right-hand side of Eq. (8).

In the slow varying amplitude approximation [25] used in this work,

$$\varepsilon_{zx} = \psi e^{i\omega_0(t - x/a_\perp)} + \text{c.c.},$$
$$\rho_{-+} = R_{-+} e^{2i\omega_0(t - x/a_\perp)}, \tag{9}$$

$$\rho_{-0} = R_{-0} e^{i\omega_0(t - x/a_\perp)},$$
$$\rho_{0+} = R_{0+} e^{i\omega_0(t - x/a_\perp)}, \tag{10}$$

where ψ and $R_{\mu\nu}$ $(\mu, \nu = -, 0, +)$ are the complex slow varying amplitudes of shear strain pulses and the off-diagonal elements of the density matrix, respectively, and ω_0 is the carrier frequency of these pulses coinciding with the central frequency of inhomogeneous broadening contours for the $- \leftrightarrow 0$ and $0 \leftrightarrow +$ transitions.

The substitution of Eqs. (9) and (10) written in the slow varying amplitude approximation into Eq. (8) yields the wave equation for the complex amplitude of signals emitted by the excited medium in the form

$$\frac{\partial \psi}{\partial x} + \frac{1}{a_\perp}\frac{\partial \psi}{\partial t} = i\frac{nG_\perp \omega_0}{16\sqrt{2}\rho a_\perp^3}\int_{-\infty}^{+\infty}(R_{0+} - R_{-0})g(\Delta)d\Delta. \tag{11}$$

Neglecting rapidly oscillating terms in the material equations and assuming that the amplitude ψ of pulses acting on the medium is real, we obtain the following equation from Eqs. (2)–(5), (9), and (10):

$$\frac{\partial R_{\mu\nu}}{\partial t} = -i(\omega_{\mu\nu}' - \omega_{\mu\nu} - i/T_{\mu\nu})R_{\mu\nu} + i\frac{G_\perp \psi}{2\sqrt{2}\hbar}\left[\hat{R}, \hat{Q}\right]_{\mu\nu}, \tag{12}$$

where

$$\hat{R} = \begin{pmatrix} \rho_{++} & R_{+0} & R_{+-} \\ R_{0+} & \rho_{00} & R_{0-} \\ R_{-+} & R_{-0} & R_{--} \end{pmatrix},$$
$$\hat{Q} = \begin{pmatrix} 0 & 1 & 0 \\ 1 & 0 & -1 \\ 0 & -1 & 0 \end{pmatrix}. \tag{13}$$

According to Eq. (13), transverse ultrasonic pulses supplied to the medium in the chosen geometry form a cascade of the $- \to 0 \to +$ quantum transitions (Fig. 1). The $- \leftrightarrow +$ transition is forbidden in this case.

3. ECHO MODES

To study echo modes, it is appropriate to divide the dynamics of the effective spins of paramagnetic ions into periods of excitation and free evolution.

Let the durations τ_p of acting pulses satisfy the condition $\tau_p \ll T_{\mu\nu}, T_{\mu\nu}^*$ $(\mu, \nu = 0, +, -)$, where $T_{\mu\nu}^*$ are the reversible phase relaxation times caused by the inhomogeneous broadening of the $\mu \leftrightarrow \nu$ quantum transitions. Correspondingly, the widths $\delta\omega_p \sim 1/\tau_p$ of pulse spectra are much larger than the inhomogeneous widths $\delta\omega \sim 1/T_{\mu\nu}^*$ of these transitions. Consequently, when describing the excitation of paramagnetic ions, the frequency detunings $\omega_{\mu\nu}' - \omega_{\mu\nu}$ from the corresponding resonances in Eq. (12) can be neglected and $T_{\mu\nu} = \infty$ can be formally set. In this case, the system (12) can be represented in the symbolic form

$$\frac{\partial \hat{R}}{\partial t} = i\frac{G_\perp \psi}{2\sqrt{2}\hbar}\left[\hat{R}, \hat{Q}\right]. \tag{14}$$

The solution of the operator equation (14) can be written in the form

$$\hat{R}(t) = \hat{U}(t, t_0)\hat{R}(t_0)\hat{U}^+(t, t_0), \tag{15}$$

where

$$\hat{U}(t, t_0) = e^{-i\hat{S}}, \; \hat{S} = \hat{Q}\frac{G_\perp}{2\sqrt{2}\hbar}\int_{t_0}^{t}\psi dt', \tag{16}$$

and t_0 is the onset time of the pulse action.

Any integer power of the matrix $\hat{Q}$ can be expressed in the form $\hat{Q}^{2k+1} = 2^k\hat{Q}$ and $\hat{Q}^{2k+2} = 2^k\hat{Q}^2$, where k is an integer. Then, the summation of the Taylor series of $e^{-i\hat{S}}$ taking into account the second of Eqs. (16) gives the evolution operator in the form

$$\hat{U}(t, t_0) = \hat{I} - \hat{Q}^2\sin^2\frac{\theta}{2} - i\frac{\hat{Q}}{\sqrt{2}}\sin\theta, \tag{17}$$

where $\hat{I}$ is the identity matrix and

$$\theta = \frac{G_\perp}{2\hbar}\int_{t_0}^{t}\psi dt'. \tag{18}$$

The integration of Eq. (12) for periods of free evolution with $\psi = 0$ provides

$$R_{-0}(t) = R_{-0}(t_1)e^{i\Delta(t - t_1)}e^{-(t - t_1)/T_{-0}},$$
$$R_{0+}(t) = R_{0+}(t_1)e^{i\Delta(t - t_1)}e^{-(t - t_1)/T_{0+}}, \tag{19}$$
$$R_{-+}(t) = R_{-+}(t_1)e^{2i\Delta(t - t_1)}e^{-(t - t_1)/T_{-+}},$$

where t_1 is the onset time of the period of free evolution.

In this case, the diagonal elements ρ_{--}, ρ_{00}, and ρ_{++} are constant.

It is important that the phase relaxation times T_{-0} and T_{0+} of the $- \leftrightarrow 0$ and $0 \leftrightarrow +$ transitions, respectively, cannot be strongly different because these transitions have the same frequency and the same spin–phonon coupling constant $G_\perp$. The difference between these phase relaxation times can be due to relaxation channels caused by the interaction of quantum transitions with the longitudinal strain field ε_{xx} and with transverse strains ε_{yx} polarized perpendicular to the magnetic field. Such phonons are related to the $- \leftrightarrow +$ transition [23, 26] (Fig. 1), which can affect the phase relaxation times T_{-0} and T_{0+}. The relaxation times T_{-0} and T_{0+} can also be slightly different because the $0 \leftrightarrow +$ transition is higher in energy than the $- \leftrightarrow 0$ transition. Summarizing, we assume the inequality

$$|T_{-0} - T_{0+}| \ll T_{-0}, T_{0+}. \tag{20}$$

Let the first ultrasonic pulse with the duration τ_1 be incident on the medium at the time $t = 0$. Then, after the time interval τ of the first period of free evolution, the medium is exposed to the second pulse with the duration τ_2. After that, at $t = \tau + \tau_1 + \tau_2$, the second period of free evolution begins where primary echo signals are formed (Fig. 2). The inequality $\tau \gg \tau_1, \tau_2$ is satisfied with a high accuracy.

Let the matrix $\hat{R}$ at $t = 0$ be determined only by the initial populations w_+, w_0, and w_- of stationary spin states of paramagnetic ions, and thereby it has the form

$$\hat{R}(0) = \begin{pmatrix} w_+ & 0 & 0 \\ 0 & w_0 & 0 \\ 0 & 0 & w_- \end{pmatrix}.$$

The application of Eqs. (15), (17), and (19) in the described sequence yields expressions for the elements of the matrix $\hat{R}$ at times $t > \tau + \tau_1 + \tau_2$.

It is seen on the right-hand side of wave equation (11) that contribution to ultrasonic response signals of the medium comes from the differences $R_{0+} - R_{-0}$, which are given by the expression

$$(R_{0+} - R_{-0})_{\text{echo}} = (R_{0+} - R_{-0})^{2\tau}_{\text{echo}} + (R_{0+} - R_{-0})^{3\tau}_{\text{echo}}, \tag{21}$$

where echo responses at times 2τ and 3τ have the form

$$(R_{0+} - R_{-0})^{2\tau}_{\text{echo}} = i f_{2\tau} e^{-i\Delta(t - 2\tau - \tau_1 - \tau_2)} e^{-(t - \tau_1 - \tau_2)/T_2}, \tag{22}$$

$$(R_{0+} - R_{-0})^{3\tau}_{\text{echo}} = i f_{3\tau} e^{-\tau/T_{-+}} \times \left(e^{-(t-\tau-\tau_1-\tau_2)/T_{0+}} - e^{-(t-\tau-\tau_1-\tau_2)/T_{-0}}\right) \times e^{-i\Delta(t - 3\tau - \tau_1 - \tau_2)}. \tag{23}$$

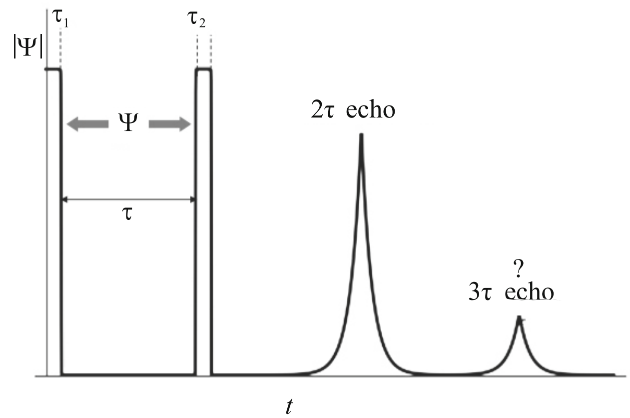

Fig. 2. Sketch of the time sequence of the exposure of the paramagnetic crystal to two transverse ultrasonic pulses with the envelope ψ and durations τ_1 and τ_2 separated by the time interval τ and the appearance of two echo signals at the times 2τ and 3τ. The appearance of 3τ echo is possible only when the irreversible phase relaxation times on $- \leftrightarrow 0$ and $0 \leftrightarrow +$ quantum transitions are different.

Here,

$$f_{2\tau} = \frac{w_- - w_+}{\sqrt{2}} \sin\theta_1 \sin^2\frac{\theta_2}{2},$$

$$f_{3\tau} = \frac{w_- - 2w_0 + w_+}{4\sqrt{2}} \sin^2\theta_1 \sin\theta_2 \sin^2\frac{\theta_2}{2}, \tag{24}$$

where $\theta_1 = \frac{G_\perp}{2\hbar}\int_0^{\tau_1} \psi dt$ and $\theta_2 = \frac{G_\perp}{2\hbar}\int_{\tau+\tau_1}^{\tau+\tau_1+\tau_2} \psi dt$ are the "areas" of the first and second exciting pulses, respectively.

The expression for $(R_{0+} - R_{-0})^{2\tau}_{\text{echo}}$ is written in the approximation $T_{-0} \approx T_{0+} = T_2$ justified by the inequality (20). The expression for $(R_{0+} - R_{-0})^{3\tau}_{\text{echo}}$ written in the same approximation has the form $(R_{0+} - R_{-0})^{3\tau}_{\text{echo}} = 0$. Consequently, the condition $T_{-0} \neq T_{0+}$ is necessary for the appearance of 3τ echo. This echo signal also disappears if phase relaxation is neglected in Eq. (23), i.e., if $T_{-0} = T_{0+} = \infty$ is formally set.

To solve the wave equation (11), we assume that distances x at which echo signals are detected are much longer than the dimension l of the paramagnetic crystal in the direction of their propagation and the medium beyond this crystal does not contain paramagnetic ions. In this case, the paramagnetic crystal can be represented at a point source at $x = 0$. Therefore, the replacement $n \to nl\delta(x)$, where $\delta(x)$ is the Dirac delta function, can be done with a high accuracy on the right-hand side of Eq. (11). Then, the product of l and the right-hand side of Eq. (11) with the replacement $t \to t - x/a_\perp$ is a solution of the inhomogeneous wave equation (11). Any medium allowing the propagation of transverse ultrasonic waves can be used as the medium surrounding the paramagnetic crystal. It is the most convenient to use an isotropic solid, where the velocity $a_\perp$ is independent of the direction of transverse wave propagation.

Summarizing the preceding paragraph and using Eqs. (22)–(24), for the times $2\tau + x/a_\perp$ and $3\tau + x/a_\perp$ at the distance x from the paramagnetic crystal, where the respective echo signals are detected, the amplitudes of the 2τ and 3τ echo signals can be obtained in the form

$$\psi_{2\tau} = -\frac{nG_\perp \omega_0 l}{32\rho a_\perp^3}\frac{\sinh\zeta}{\cosh\zeta + 1/2}\sin\theta_1 \sin^2\frac{\theta_2}{2}e^{-2\tau/T_2}, \quad (25)$$

$$\psi_{3\tau} = -\frac{nG_\perp \omega_0 l}{128\rho a_\perp^3}\frac{\cosh\zeta - 1}{\cosh\zeta + 1/2} \times \sin^2\theta_1 \sin\theta_2 \sin^2\frac{\theta_2}{2}e^{-\tau/T_{-+}}(e^{-2\tau/T_{0+}} - e^{-2\tau/T_{-0}}), \quad (26)$$

where $\zeta = \hbar\omega_0/k_B T$, k_B is the Boltzmann constant, and T is the temperature of the paramagnetic crystal. Here, the Boltzmann distribution of the initial populations of spin sublevels was used.

We focus on the 3τ echo signal. As stated above, phase relaxation is fundamentally necessary for the appearance of an echo signal at the time $3\tau + x/a_\perp$. According to Eq. (26), relaxation times of the $- \leftrightarrow 0$ and $0 \leftrightarrow +$ transitions should be different. This conclusion is nontrivial because phase relaxation suppresses the coherence of atomic states that is necessary for the generation of any echo signals. At the same time, just phase relaxation ensures the generation of the coherent echo signal in the considered case.

The appearance of 3τ echo is physically due to the destructive interference of the $- \leftrightarrow 0$ and $0 \leftrightarrow +$ quantum transitions at the time $t = 3\tau + x/a_\perp$. If these transitions have the identical parameters, the echo response is completely suppressed. However, the identity of the parameters is violated because these transitions have different phase relaxation times. As a result, coherence generated in one of the transition decays more rapidly, which leads to an incomplete compensation of coherences of both transitions.

It is noteworthy that the $- \leftrightarrow 0$ and $0 \leftrightarrow +$ transitions have the same frequency; i.e., the three-level medium with the cascade of allowed quantum transitions is equidistant (Fig. 1). Consequently, antiphase coherences at both transitions reach maxima at the same time $t = 3\tau + x/a_\perp$. The corresponding times in the nonequidistant medium would be separated by an interval determined by the difference between the frequencies of the considered transitions [14].

We note that the interference of the $- \leftrightarrow 0$ and $0 \leftrightarrow +$ quantum transitions at the time $t = 2\tau + x/a_\perp$ is constructive (coherences generated in both transitions are in-phase). Therefore, these transitions enhance rather than suppress each other when generating 2τ echo. Just for this reason, $T_{-0} \approx T_{0+} = T_2$ can be set in Eq. (22) without loss of generality.

According to Eq. (26), the amplitude of the 3τ echo signal is maximal at areas of the exciting pulses $\theta_1 = \pi/2$ and $\theta_2 = 2\pi/3$. Choosing the areas of the exciting pulses, one cannot suppress the 2τ echo signal to observe only the 3τ echo signal. Furthermore, as follows from Eqs. (25) and (26) taking into account Eq. (20), the intensity of 3τ echo is much lower than that of 2τ echo (see Fig. 2).

For the possible experimental implementation of the considered spin–phonon echo, numerical estimates are obtained below for a MgO crystal sample at liquid helium temperatures with incorporated Fe^{2+} paramagnetic ions [22, 23]. The reversible phase relaxation times for quantum transitions between Zeeman sublevels of Fe^{2+} ions in the crystal MgO, as well as the characteristic durations of echo signals, are $T^*_{\mu\nu} \sim 10^{-7}$ s [23, 27]. To satisfy the above condition $\tau_p \ll T^*_{\mu\nu}$, the duration of exciting pulses should be $\tau_p \sim 10^{-8}$ s. Taking the irreversible phase relaxation times $T_{-0} \sim T_{-+} \sim 10^{-5}$ s [10, 22, 23], we assume $\tau \sim 10^{-5}$ s for the time delay between two exciting pulses. The carrier frequency of the pulses is $\omega_0 \sim 10^{11}$ s^{-1} [10, 22, 23]. Taking $a_\perp = 3\times10^5$ cm/s for the speed of transverse ultrasound [10, 28] and $D \approx l \sim 1$ mm for the aperture D of the pump pulses and echo signals, we estimate the characteristic length of diffraction broadening of the pulse $l_D \sim \omega_0 D^2/a_\parallel \sim 10^2$–$10^3$ cm. This value is much larger than the considered spatial scales and, hence, is in good agreement with the one-dimensional approximation used in Eq. (11). Thus, echo signals can be detected using the corresponding detectors placed at distances of several centimeters from the sample.

The spin–phonon coupling constant can be estimated at $G_\perp \sim 10^{-14}$ erg. Then, the amplitude of strains induced by the pulses incident on the medium is $\psi \sim \hbar/G_\perp\tau_p \sim 10^{-5}$. Let $l \sim 1$ mm, $T \sim 1$ K, $n \sim 10^{19}$ cm^{-3}, and $\rho = 3.6$ g/cm^3 [10, 22, 23]. Since the difference between the times T_{-0} and T_{0+} is small, we can set $e^{-\tau/T_{-+}}(e^{-2\tau/T_{0+}} - e^{-2\tau/T_{-0}}) \sim 10^{-2}$, and the amplitudes of the 2τ and 3τ echo signals can be estimated as $|\psi_{2\tau}| \sim 10^{-5}$ and $|\psi_{3\tau}| \sim 10^{-7} \ll |\psi_{2\tau}|$ from Eqs. (25) and (26), respectively, using the above estimates for ω_0, $a_\perp$, and l. Such amplitudes of the strain can certainly be detected in real experiments [10, 22].

Here, a fundamental question is whether irreversible phase relaxation times at two transitions can be different, although these transitions have the same frequency and the same spin–phonon coupling constant. In this case, if the answer is positive, the 3τ echo signal can appear. Therefore, the detection of the discussed rather weak echo signal in an actual experiment can provide information on the relation between coherence relaxation times of allowed quantum transitions. If this echo signal is not detected in the actual experiment, this will be a serious reason for the conclusion that relaxation times of the corresponding allowed transitions coincide with each other. If this echo signal is detected, the difference between the discussed relaxation times can be determined from the intensity of the signal.

4. CONCLUSIONS

To summarize, it has been demonstrated that the generation of a coherent echo signal caused by irreversible phase relaxation in an equidistant three-layer system with a cascade of allowed transitions is possible. Correspondingly, the discussed echo signal hardly has an optical analog because physical implementations of equidistant three-level systems with the cascade of quantum transitions apparently do not exist in the optical range. Here, ultrasonic echo in the system of paramagnetic ions incorporated in a cubic crystal has been considered as a physical implementation.

It seems important that incoherent processes in the medium are responsible for the appearance of one of the coherent responses of the medium to an external resonant action. This effect is impossible in the two-level system because it is due to the destructive interference of two quantum transitions emitting in antiphase.

CONFLICT OF INTEREST

The author declares that he has no conflicts of interest.

OPEN ACCESS

REFERENCES

1. U. Kh. Kopvillem and V. R. Nagibarov, Fiz. Met. Metalloved. **15**, 313 (1963).
2. N. A. Kurnit, I. D. Abella, and S. R. Hartmann, Phys. Rev. Lett. **6**, 567 (1964).
3. V. V. Samartsev, V. A. Zuikov, and L. A. Nefed'ev, Zh. Prikl. Spektrosk. **59**, 395 (1993).
4. E. A. Manykin and V. V. Samartsev, *Optical Echo Spectroscopy* (Nauka, Moscow, 1984) [in Russian].
5. E. L. Hahn, Phys. Rev. **80**, 580 (1950).
6. N. M. Pomerantsev, Usp. Fiz. Nauk **65**, 87 (1958).
7. V. R. Nagibarov and U. Kh. Kopvillem, Sov. Phys. JETP **25**, 618 (1967).
8. N. S. Shiren and I. G. Kazyaka, Phys. Rev. Lett. **28**, 1304 (1972).
9. D. R. Taylor and I. G. Bartlet, Phys. Rev. Lett. **30**, 96 (1973).
10. V. A. Golenishchev-Kutuzov, V. V. Samartsev, N. K. Solovarov, and B. M. Khabibullin, *Magnetic Quantum Acoustics* (Nauka, Moscow, 1977) [in Russian].
11. A. M. Shegeda, S. L. Korableva, O. A. Morozov, V. N. Lisin, N. K. Solovarov, and V. F. Tarasov, JETP Lett. **117** (2023, in press).
12. R. Beah and S. R. Hartmann, Phys. Rev. Lett. **53**, 663 (1984).
13. S. Asaka, H. Nakatsuka, M. Fujiwara, and M. A. Matsuoka, Phys. Rev. A **29**, 2286 (1984).
14. A. Yu. Parkhomenko and S. V. Sazonov, JETP Lett. **67**, 934 (1998).
15. N. V. Znamenskii and S. V. Sazonov, JETP Lett. **85**, 358 (2007).
16. R. M. Arkhipov, M. V. Arkhipov, and N. N. Rosanov, JETP Lett. **111**, 484 (2020).
17. J. E. Golub and T. W. Mossberg, J. Opt. Soc. Am. B **3**, 554 (1986).
18. V. V. Samartsev, A. M. Shegeda, A. V. Shkalikov, K. R. Karimullin, T. G. Mitrofanova, and V. A. Zuikov, Laser Phys. Lett. **4**, 534 (2007).
19. V. N. Lisin, A. M. Shegeda, V. V. Samartsev, and E. P. Chukalina, JETP Lett. **107**, 345 (2018).
20. V. V. Fedyanin and K. R. Karimullin, Izv. Akad. Nauk, Ser. Fiz. **84**, 361 (2020).
21. V. V. Fedyanin and K. R. Karimullin, Laser Phys. **29**, 124008 (2019).
22. J. W. Tucker and V. W. Rampton, *Microwave Ultrasonics in Solid State Physics* (North-Holland, Amsterdam, 1972).
23. N. S. Shiren, Phys. Rev. B **2**, 2471 (1970).
24. S. V. Sazonov, J. Phys.: Condens. Matter **6**, 6295 (1994).
25. L. Allen and J. H. Eberly, *Optical Resonance and Two-Level Atoms* (Wiley, New York, 1975).
26. S. V. Sazonov, J. Exp. Theor. Phys. **117**, 885 (2013).
27. U. Kh. Kopvillem and V. R. Rizaev, Sov. Phys. JETP **38**, 1147 (1974).
28. G. Kino, *Acoustic Waves: Devices, Imaging, and Analog Signal Processing* (Prentice-Hall, New Jersey, 1987).

Translated by R. Tyapaev